18 - volume growth
cardiac growth

day	date		topic
tue	jan	07	motivation - everything grows!
thu	jan	09	basics maths - notation and tensors
tue	jan	14	project example - growing skin
thu	jan	16	kinematics - growing brains
tue	jan	21	basic kinematics - large deformation and growth
thu	jan	23	kinematics - growing hearts
tue	jan	28	balance equations - closed and open systems
thu	jan	30	balance equations - wound healing
tue	feb	04	basic constitutive equations - growing muscle
thu	feb	06	basic constitutive equations - growing tumors
tue	feb	11	volume growth - finite elements for growth - theory
thu	feb	13	volume growth - finite elements for growth - matlab
tue	feb	18	basic constitutive equations - growing bones
thu	feb	20	density growth - finite elements for growth
tue	feb	25	density growth - growing wounds
thu	feb	27	everything grows! - midterm summary
tue	mar	04	midterm
thu	mar	06	volume growth - growing hearts
tue	mar	11	class project - discussion, presentation, evaluation
thu	mar	13	no class - work on final project reports
fri	mar	15	final project reports due

ME 337 – Mechanics of Growth

Instructions for Judges
according to ASME / SBC conference review guidelines

The presentation format includes the **structure of the presentaiton and its composition**. In general, a presentation should be structured to include an introduction, method, analysis, results, a conclusion, and references. The introduction should define the problem, scope of the study, and a brief background of previous work. The method section also should be brief to leave the majority of the report body for results and discussion. The final paragraph should be a brief paragraph on inference or conclusions reached.

Technical merit should be judged on the completeness of what is reported. For scientific studies, the result should support the conclusions presented. The key is validation of the express conclusion with results and data. Unsubstantiated conclusions or results should receive minimum points. However, not all papers represent basic research. Some papers present the design of a hardware system or a new software development. Both require the development of tests and measurement procedures to validate the product.

After the scoring is complete, please indicate a final grade. Please provide a comment in the designated area that describes why you think this presentation suitable/not suitable. These comments will be collected and provide to the students for feedback.

ME 337 – Mechanics of Growth

Is not necessary for the judge to be an expert in the field represented by the paper to evaluate its technical merit using these criteria. Subjective rating of the paper's scientific contribution is not encouraged unless there is evidence that the conclusions are incorrect. A judge should feel free to consult colleagues who are experts in the field, if you are unsure about the correctness of the conclusions. Since presentations can vary from hardware designs to software technique, or simulations and modeling to basic research, each reviewer will have to use his/her own best judgment about the technical merit of the work that is presented.

Scoring & Evaluation System:

Please use the same scoring system as for the General Abstracts for each of the evaluation categories.

Score – Provide a ranking according to

Excellent	= 100
Very Good	= 90
Good	= 80
Marginal	= 60
Poor	= 50

Evaluation Categories

1. Structure of presentation
2. Technical merit
3. Style of presentation

Keep in mind the judges cannot be perfect, but will try to be consistent in scoring. There are multiple judges for

heart disease

- primary cause of death in industrialized nations
- affects 80 mio americans
- damaged cardiac tissue does not self regenerate

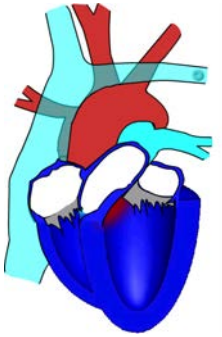

forms of cardiac growth

- case I - athlete's heart
  stress driven isotropic growth
- case II - cardiac dilation
  strain driven eccentric growth
- case III - cardiac wall thickening
  stress driven concentric growth

organ level - human heart and its characteristic microstructure

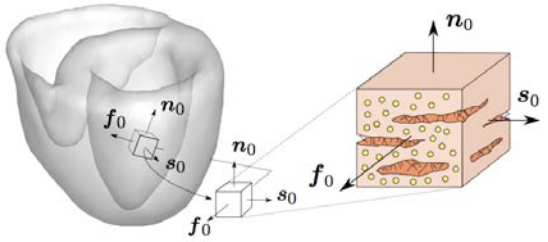

Figure 1. Normal healthy heart, courtesy of Chengpei Xu (left). Microstructural architecture of the heart (right). The orthogonal unit vectors f_0 and s_0 designate the muscle fiber direction and the sheet plane vector in the undeformed configuration. The orthogonal vector n_0 completes the local coordinate system, where the constitutive response of the heart is typically viewed as orthotropic.

goktepe, abilez, kuhl [2010]

cellular level - cardiomyocyte and its characteristic microstructure

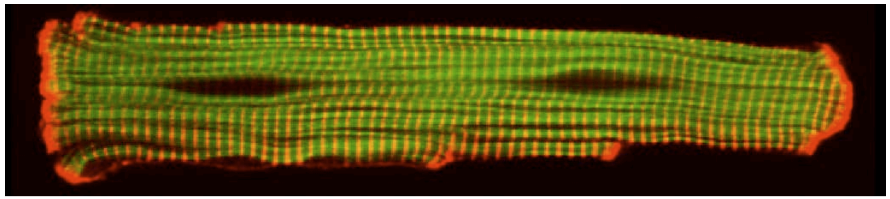

Figure 1. Adult ventricular cardiomyocyte. The sarcomeric actin is labeled in green and the periodically spaced t-tubule system is marked in red, giving the cell its characteristic striated appearance. Healthy cardiomyocytes have a cylindrical shape with a diameter of 10-25μm and a length of 100μm, consisting of approximately 50 sarcomere units in series making up a myofibril and 50-100 myofibrils in parallel. Cardiac disease can be attributed to structural changes in the cardiomyocyte, either through eccentric growth in dilated cardiomyopathy or through concentric growth in hypertrophic cardiomyopathy.

kevin kit parker, disease biophysics group, harvard

molecular level - sarcomere and its characteristic microstructure

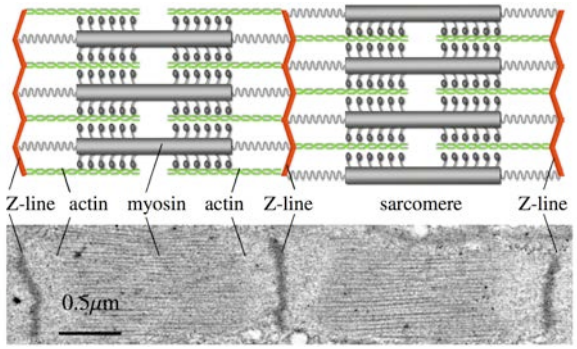

Figure 2. Sarcomere units of human embryonic stem cell-derived cardiomyocyte. Sarcomeres are defined as the segment between two neighboring Z-lines, shown in red, which appear as dark lines under the transmission electron microscope. Healthy sarcomeres are 1.9-2.1μm long characterized through a parallel arrangement of thick filaments of myosin, displayed in grey, sliding along thin filaments of actin, labeled in green. Although cardiac cells are known to change length and thickness in response to mechanical loading, the individual sarcomeres maintain an optimal resting length.

goktepe, abilez, parker, kuhl [2010]

organ level - pathophysiology of maladaptive growth

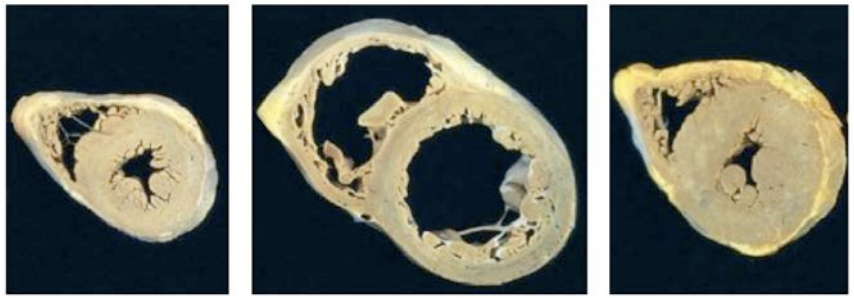

Figure 2. Pathophysiology of maladaptive growth of the heart viewed in transverse heart sections, reprinted with permission from Robbins & Cotran. Compared with the normal heart (left), eccentric hypertrophy is associated with ventricular dilation in response to volume overload (center). Concentric hypertrophy is associated with ventricular wall thickening in response to pressure overload (right).

kumar, abbas, fausto [2005]

cellular level - pathophysiology of maladaptive growth

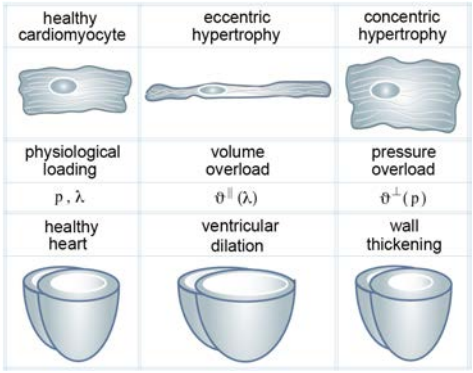

Figure 3. Eccentric and concentric growth on the cellular and organ levels. Compared with the normal heart (left), volume-overload induced eccentric hypertrophy is associated with cell lengthening through the serial deposition of sarcomere units and manifests itself in ventricular dilation in response to volume-overload (center). Pressure-overload induced concentric hypertrophy is associated with cell thickening through the parallel deposition of sarcomere units and manifests itself in ventricular wall thickening in response to pressure-overload (right).

goktepe, abilez, parker, kuhl [2010]

molecular level - pathophysiology of maladaptive growth

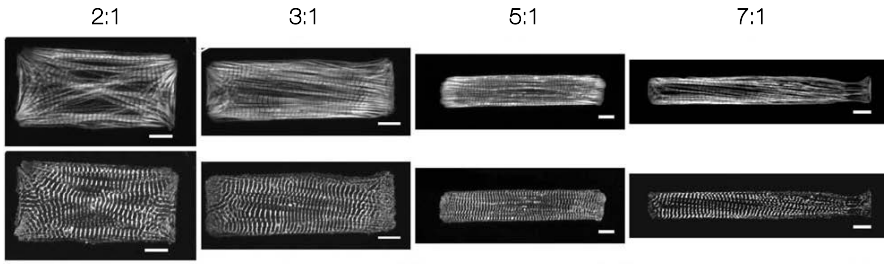

Figure 3.Controlled cardiomyocyte remodeling in vitro. Cardiomyocytes adapt their size, shape, and intracellular architecture when spatially confined in vitro through patterning on fibronactin islands at different aspect ratios (2:1, 3:1, 5:1, and 7:1). Isolated confocal slices display 2D morphology of myofibrils with respect to actin (top) and alpha-actinin (bottom). Although overall cardiomyocyte size changes, the individual sarcomere units remain at constant length.

geisse, sheehy, parker [2009]

linking growth across the scales - fiber orientation

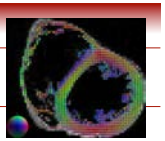

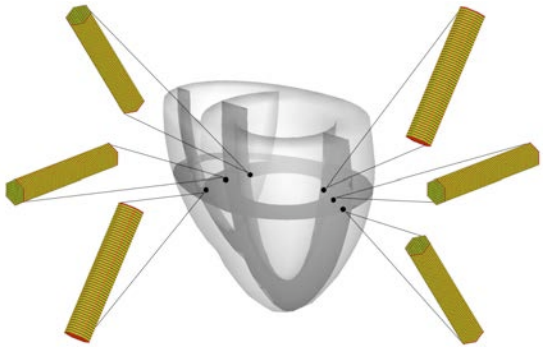

Figure 6. Generic biventricular heart model generated from two truncated ellipsoids, with heights of 70mm and 60mm, radii of 30mm and 51mm, and wall thicknesses of 12mm and 6mm, respectively. In the healthy heart, cardiomyocytes are assumed to be cylindrical, 100µm long with a diameter of 16.7µm. They consist of 50 serial sarcomere units in length and 91 parallel units per cross section, each of them 2µm long and 2µm in diameter. They are arranged helically around the long axis of the heart with a transmurally varying inclination of -55º in the epicardium, the outer wall, to +55º in the endocardium, the inner wall, measured with respect to the basal plane.

goktepe, abilez, parker, kuhl [2010], collaboration with dan ennis, dept radiology, UCLA

kinematics of finite growth

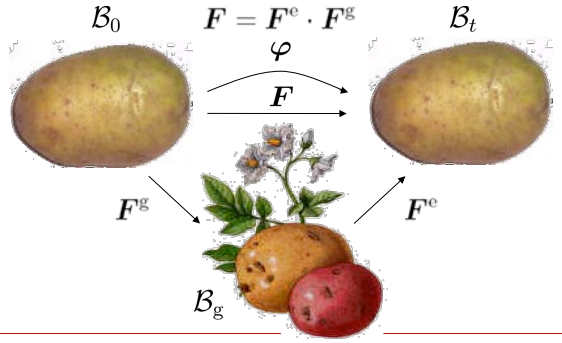

concept of incompatible growth configuration

lee [1969], rodriguez, hoger, mc culloch [1994], taber [1995], epstein, maugin [2000], humphrey [2002], ambrosi, mollica [2002], himpel, kuhl, menzel, steinmann [2005]

motivation - cardiac growth

locally orthotropic material behavior

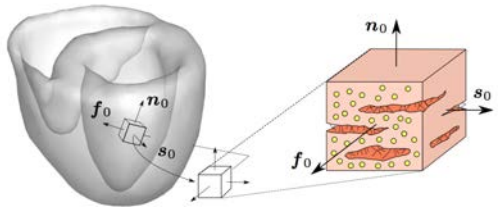

$$\psi = \kappa\,[J^{\mathrm{e}} - \ln(J^{\mathrm{e}}) - 1] + \frac{a}{2b}\,\exp(b[I_1^{\mathrm{e}} - 3])$$
$$+ \frac{a_{\mathrm{s}}}{2b_{\mathrm{s}}}[\exp(b_{\mathrm{s}}[I_{\mathrm{s}}^{\mathrm{e}} - 1]^2) - 1] + \frac{a_{\mathrm{f}}}{2b_{\mathrm{f}}}[\exp(b_{\mathrm{f}}[I_{\mathrm{f}}^{\mathrm{e}} - 1]^2) - 1] + \frac{a_{\mathrm{fs}}}{2b_{\mathrm{fs}}}[\exp(b_{\mathrm{fs}}\, I_{\mathrm{fs}}^{\mathrm{e}\,2}) - 1]$$

$$\boldsymbol{\tau} = 2\frac{\partial \psi}{\partial \boldsymbol{g}} = J^{\mathrm{e}}\, p\, \boldsymbol{g}^{-1} + 2\,\psi_1'\ \boldsymbol{b}^{\mathrm{e}} + 2\,\psi_{\mathrm{f}}'\ \boldsymbol{f}^{\mathrm{e}} \otimes \boldsymbol{f}^{\mathrm{e}}$$
$$+ 2\,\psi_{\mathrm{fs}}'[\boldsymbol{f}^{\mathrm{e}} \otimes \boldsymbol{s}^{\mathrm{e}}]^{\mathrm{sym}} + 2\,\psi_{\mathrm{s}}'\ \boldsymbol{s}^{\mathrm{e}} \otimes \boldsymbol{s}^{\mathrm{e}}$$

dokos, smaill, young, le griece [2002], schmid, nash, young, hunter [2006]. holzapfel, ogden [2009], göktepe, acharya, wong, kuhl [2010]

constitutive equations

locally orthotropic material behavior

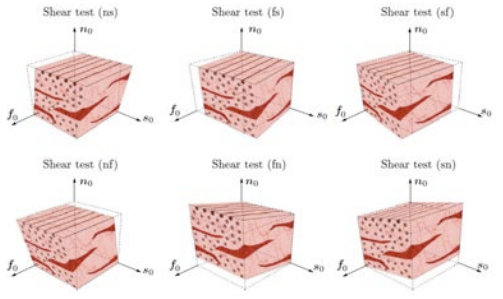

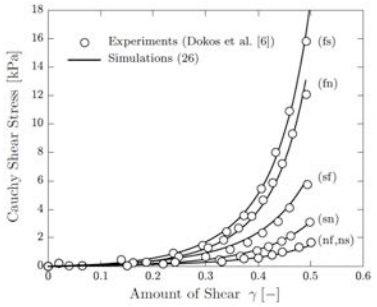

dokos, smaill, young, le griece [2002], schmid, nash, young, hunter [2006]. holzapfel, ogden [2009], göktepe, acharya, wong, kuhl [2010]

constitutive equations

locally orthotropic material behavior

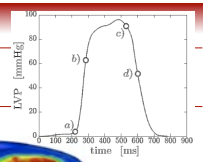

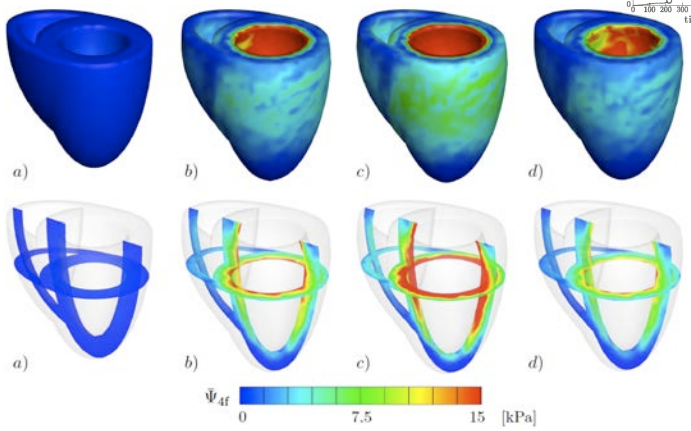

göktepe, acharya, wong, kuhl [2010]

constitutive equations

case I - athlete's heart syndrome

- growth due to **significant exercise**
- driven by **elevated pressure** and **increased filling**

- cardiac **output increases** from 6 l/min at rest **to 40 l/min**
- cardiac **mass increases** up to **50%**

- cardiomyocyte number remains constant ~6 billion
- cardiomyocyte **size increases isotropically up to 40%**

eckblom, hermansen [1968], hunter, chien [1999], plum, zwinderman, van der laarse, van der wall [2000]

first reported case of heart failure in athletes

the word **marathon** originates from the **legend of phidippides**. phidippides was sent from the battlefield of marathon to athens to announce that the persians who had invaded greece had been defeated in the battle of marathon. the legend states that phidippides ran the entire **distance of 26 miles** without stopping and burst into the assembly, to announce greece's victory before he **collapsed and died on the spot**. [490bc]

physiology of athlete's heart

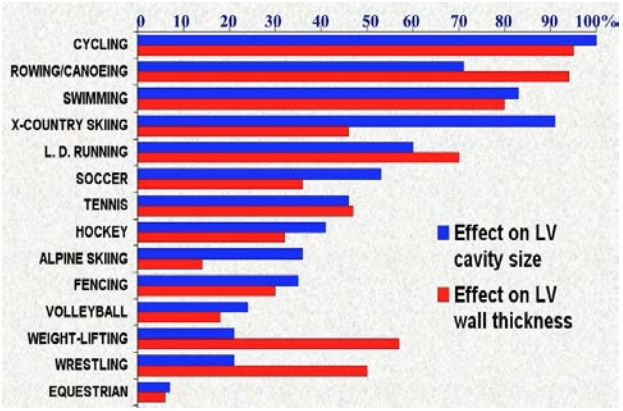

Table. Relative impact of different sports on left ventricular (LV) dimensions.

pelliccia [1998]

governing equations

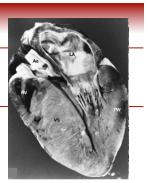

- multiplicative decomposition
  $\boldsymbol{F} = \boldsymbol{F}^{\mathrm{e}} \cdot \boldsymbol{F}^{\mathrm{g}}$ with $\boldsymbol{F} = \nabla_{\boldsymbol{X}} \boldsymbol{\varphi}$
- growth tensor
  $\boldsymbol{F}^{\mathrm{g}} = \vartheta^{\mathrm{g}} \boldsymbol{I}$
- evolution of isotropic growth multiplier
  cardiomyocyte volume increase rate
  $\dot{\vartheta}^{\mathrm{g}} = k^{\mathrm{g}}(\vartheta^{\mathrm{g}})\, \phi^{\mathrm{g}}(\boldsymbol{M}^{\mathrm{e}})$ with $k^{\mathrm{g}}(\vartheta^{\mathrm{g}}) = \frac{1}{\tau}\left[\frac{\vartheta^{\max} - \vartheta^{\mathrm{g}}}{\vartheta^{\max} - 1}\right]^{\gamma}$
- growth criterion
  $\phi^{\mathrm{g}} = \mathrm{tr}(\boldsymbol{M}^{\mathrm{e}}) - M^{\mathrm{e\,crit}}$

maximum cardiomyocyte increase $\vartheta^{\max}$, sarcomere deposition time τ, deposition nonlinearity γ, critical pressure level $M^{\mathrm{e\,crit}}$

four parameter growth model - sensitivity analysis

$$\phi^{g} = \mathrm{tr}(\boldsymbol{M}^{e}) - M^{e\,crit} \qquad k^{g}(\vartheta^{g}) = [[\vartheta^{max} - \vartheta^{g}] / [\vartheta^{max} - 1]]^{\gamma} / \tau$$

maximum cardiomyocyte increase ϑ^{max} sarcomere deposition time τ

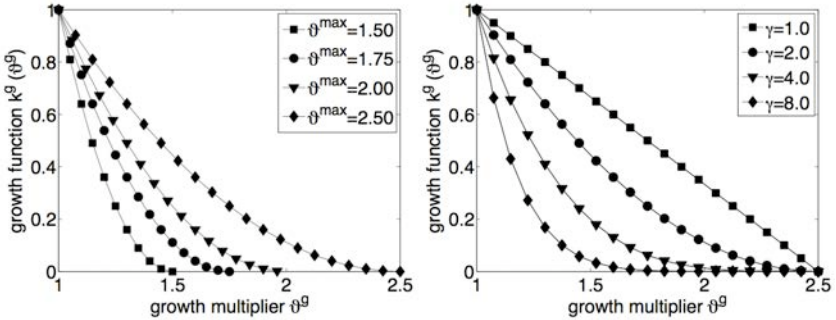

Figure 5. Three-parameter growth function. The growth rate decays smoothly until the growth multiplier ϑ has reached its maximum value ϑ^{max}, here shown for $\gamma = 2.0$ and $\tau = 1.0$ (left). The nonlinearity of the growth process increases for increasing γ, here shown for $\gamma = 2.5$ and $\tau = 1.0$.

göktepe, abilez, kuhl [2010]

algorithmic treatment

given $\boldsymbol{F}$ and ϑ^{g}_{n}	
initialize $\vartheta^{g} \leftarrow \vartheta^{g}_{n}$	
local Newton iteration	
calculate elastic tensor $\boldsymbol{F}^{e} = \boldsymbol{F} / \vartheta^{g}$	(1)
calculate elastic right Cauchy Green tensor $\boldsymbol{C}^{e} = \boldsymbol{F}^{e\,t} \cdot \boldsymbol{F}^{e}$	(2)
calculate second Piola Kirchhoff stress $\boldsymbol{S}^{e} = 2\,\partial\psi / \partial\boldsymbol{C}^{e}$	(10)
check growth criterion $\phi^{g} = \mathrm{tr}(\boldsymbol{C}^{e} \cdot \boldsymbol{S}^{e}) - M^{e\,crit} \geq 0$?	(29)
calculate growth function $k^{g} = [[\vartheta^{max} - \vartheta^{g}]/[\vartheta^{max} - 1]]^{\gamma} / \tau$	(28)
calculate residual $\mathsf{R} = \vartheta^{g} - \vartheta^{g}_{n} - k^{g}\,\phi^{g}\Delta t$	(30)
calculate tangent $\mathsf{K} = \partial\mathsf{R} / \partial\vartheta^{g}$	(31)
update growth multiplier $\vartheta^{g} \leftarrow \vartheta^{g} - \mathsf{R} / \mathsf{K}$	
check convergence $\mathsf{R} \leq \mathrm{tol}$?	
calculate second Piola Kirchhoff stress $\boldsymbol{S} = 1 / \vartheta^{g\,2}\,\boldsymbol{S}^{e}$	(32)
calculate Lagrangian moduli $\mathbf{L}$	(35)
push forward to Kirchhoff stresses $\boldsymbol{\tau} = \boldsymbol{F} \cdot \boldsymbol{S} \cdot \boldsymbol{F}^{t}$	(36)
push forward to Eulerian moduli $\mathbf{e} = [\boldsymbol{F} \otimes \boldsymbol{F}] : \mathbf{L} : [\boldsymbol{F}^{t} \otimes \boldsymbol{F}^{t}]$	(37)

Table 1. Algorithmic treatment of stress-driven isotropic growth.

göktepe, abilez, kuhl [2010]

physiology of athlete's heart syndrome

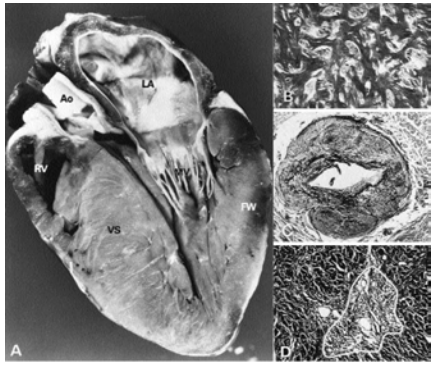

Figure. Morphological components of the disease process in hypertrophic cardiomyopathy (HCM), the most common cause of sudden death in young competitive athletes. A. Gross heart specimen sectioned in cross-sectional plane; left ventricular wall thickening shows an asymmetrical pattern and is confined primarily to the ventricular septum, which bulges prominently into the left ventricular outflow tract. the levt ventricular cavity appears in reduced size. B-D Histological features characteristic of left ventricular myocardium in HCM.

maron [1997]

athlete's heart - stress-driven isotropic growth

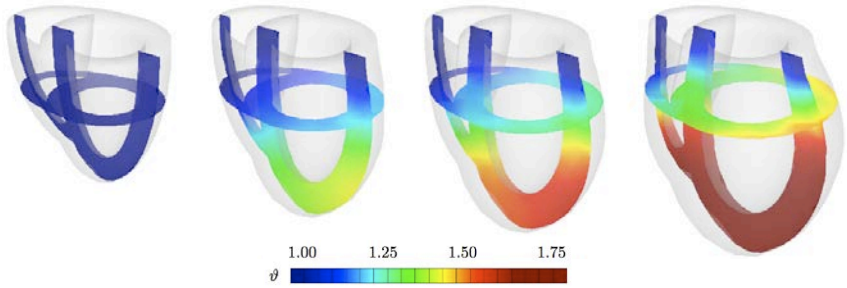

Figure 7. Athlete's heart, stress-driven isotropic eccentric and concentric growth, left ventricular dilation and wall thickening. The isotropic growth multiplier gradually increases from 1.00 to 1.75 as the individual cardiomyocytes grow both eccentrically and concentrically. On the macroscopic scale, the athlete's heart manifests itself in a progressive apical growth with a considerably increase in left ventricular cavity size to enable increased cardiac output during excercise. To withstand higher blood pressure levels during training, the heart muscle grows and the wall thickens.

göktepe, abilez, kuhl [2010]

case II - cardiac dilation

- chronic **enlargement** at constant wall thickness
- cardiac **mass increases 3x** to 1000 g
- cardiomyocyte number remains constant ~6 billion
- cardiomyocytes **lengthen 40%** at constant cell diameter
- sarcomere number increases **from ~50 to ~70** in series
- sarcomere length remains constant at 1.9-2.1um

ackblom, hermansen [1968], gerdes et al [1992], hunter, chien [1999], plum et al [2000], yoshida et al [2010]

case II - cardiac dilation

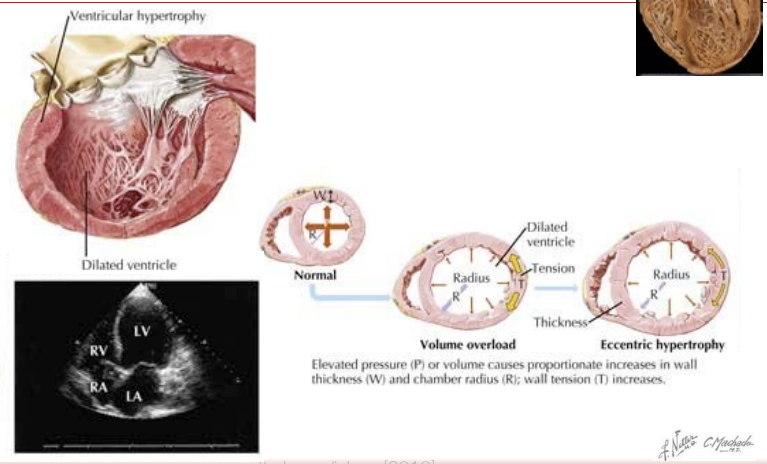

netter's cardiology [2010]

constitutive equations

- multiplicative decomposition

$$\boldsymbol{F} = \boldsymbol{F}^{\mathrm{e}} \cdot \boldsymbol{F}^{\mathrm{g}} \qquad \text{with} \quad \boldsymbol{F} = \nabla_{\boldsymbol{X}} \boldsymbol{\varphi}$$

- growth tensor

$$\boldsymbol{F}^{\mathrm{g}} = \boldsymbol{I} + [\,\lambda^{\mathrm{g}} - 1\,]\, \boldsymbol{f}_0 \otimes \boldsymbol{f}_0$$

- evolution of eccentric growth multiplier
  serial sarcomere deposition rate

$$\dot{\lambda}^{\mathrm{g}} = k^{\mathrm{g}}(\lambda^{\mathrm{g}})\, \phi^{\mathrm{g}}(\lambda^{\mathrm{e}}) \qquad \text{with} \quad k^{\mathrm{g}} = \frac{1}{\tau} \left[\frac{\lambda^{\max} - \lambda^{\mathrm{g}}}{\lambda^{\max} - 1} \right]^{\gamma}$$

- growth criterion

$$\phi^{\mathrm{g}} = \lambda^{\mathrm{e}} - \lambda^{\mathrm{crit}} = \frac{\lambda}{\lambda^{\mathrm{g}}} - \lambda^{\mathrm{crit}}$$

maximum serial sarcomere deposition $\lambda^{\max}$, sarcomere deposition time τ, deposition nonlinearity γ, critical sarcomere stretch λ^{crit}

algorithmic treatment

given $\boldsymbol{F}$ and $\lambda^{\mathrm{g}}_{\mathrm{n}}$	
initialize $\lambda^{\mathrm{g}} \leftarrow \lambda^{\mathrm{g}}_{\mathrm{n}}$	
local Newton iteration	
check growth criterion $\phi^{\mathrm{g}} = \lambda^{\mathrm{e}} - \lambda^{\mathrm{crit}} \geq 0$?	(46)
calculate growth function $k^{\mathrm{g}} = [[\lambda^{\max} - \lambda^{\mathrm{g}}]/[\lambda^{\max} - 1]]^{\gamma} / \tau$	(45)
calculate residual $\mathsf{R} = \lambda^{\mathrm{g}} - \lambda^{\mathrm{g}}_{\mathrm{n}} - k^{\mathrm{g}}\, \phi^{\mathrm{g}} \Delta t$	(47)
calculate tangent $\mathsf{K} = \partial \mathsf{R} / \partial \vartheta^{\mathrm{g}}$	(48)
update growth stretch $\lambda^{\mathrm{g}} \leftarrow \lambda^{\mathrm{g}} - \mathsf{R} / \mathsf{K}$	
check convergence $\mathsf{R} \leq$ tol ?	
calculate growth tensor $\boldsymbol{F}^{\mathrm{g}} = \boldsymbol{I} + [\lambda^{\mathrm{g}} - 1] \boldsymbol{f}_0 \otimes \boldsymbol{f}_0$	(41)
calculate elastic tensor $\boldsymbol{F}^{\mathrm{e}} = \boldsymbol{F} \cdot \boldsymbol{F}^{\mathrm{g}\,-1}$	(1)
calculate elastic right Cauchy Green tensor $\boldsymbol{C}^{\mathrm{e}} = \boldsymbol{F}^{\mathrm{e}\,\mathrm{t}} \cdot \boldsymbol{F}^{\mathrm{e}}$	(2)
calculate elastic second Piola Kirchhoff stress $\boldsymbol{S}^{\mathrm{e}} = 2\, \partial \psi / \partial \boldsymbol{C}^{\mathrm{e}}$	(10)
calculate second Piola Kirchhoff stress $\boldsymbol{S} = \boldsymbol{F}^{\mathrm{g}\,-1} \cdot \boldsymbol{S}^{\mathrm{e}} \cdot \boldsymbol{F}^{\mathrm{g}}$	(17)
calculate Lagrangian moduli L	(18) with (19), (20), (43), (49)
push forward to Kirchhoff stress $\boldsymbol{\tau} = \boldsymbol{F} \cdot \boldsymbol{S} \cdot \boldsymbol{F}^{\mathrm{t}}$	(21)
push forward to Eulerian moduli $\mathbf{e} = [\boldsymbol{F} \,\overline{\otimes}\, \boldsymbol{F}] : \mathsf{L} : [\boldsymbol{F}^{\mathrm{t}} \,\overline{\otimes}\, \boldsymbol{F}^{\mathrm{t}}]$	(22)

Table 2. Algorithmic treatment of strain-driven transversely isotropic growth.

göktepe, abilez, kuhl [2010]

pathophysiology of cardiac dilation

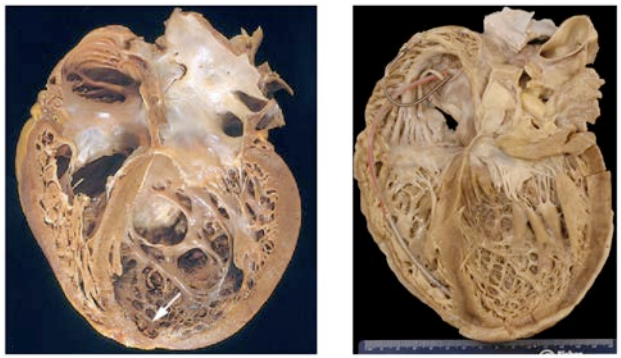

Figure 8. Strain-driven eccentric growth, cardiac dilation, and increase in cavity size at constant wall thickness. The heart is usually enlarged, rounded, flabby, and heavy with a weight of up to three times its normal weight (left), reprinted with permission from Robbins and Cotran. Heart specimen from a patient with cardiac dilation who died in end-stage heart failure. The ventricles are significantly dilated while the wall thickness has remained unaltered, courtesy of Allen P. Burke.

cardiac dilation through strain-driven eccentric growth

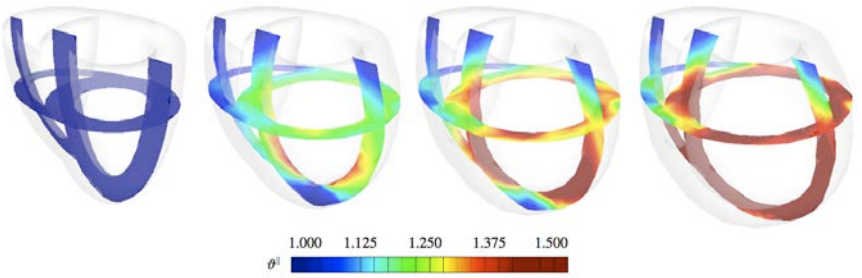

Figure 10. Strain-driven eccentric growth. The eccentric growth multiplier gradually increases from 1.00 to 1.50 as the individual cardiomyocytes grow eccentrically. On the structural level, eccentric growth manifests itself in a progressive dilation of the left ventricle accompanied by a significant increase in cardiac mass, while the thickness of the ventricular wall remains virtually unchanged.

cardiac dilation through strain-driven eccentric growth

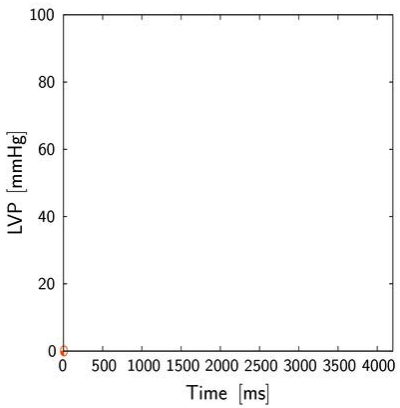

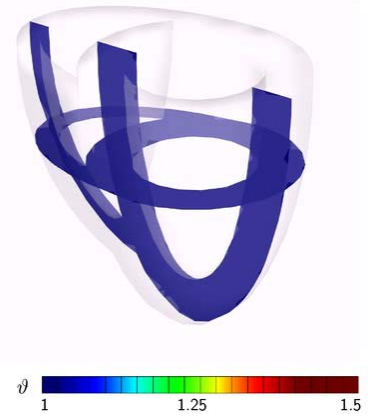

in vivo model of cardiac dilation

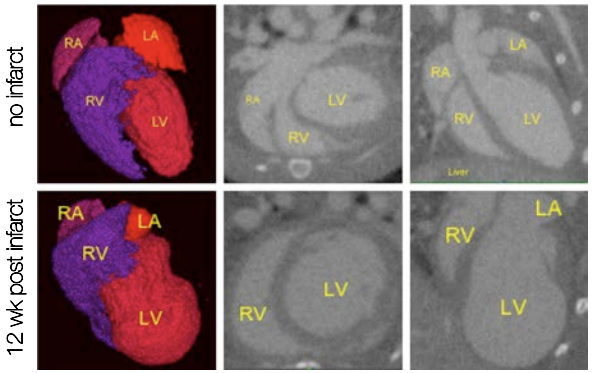

end-diastolic volume ↑ from 37.12mm^3 to 133.16mm^3

doyle, sheikh, sheikh, cao, yang, robbins, wu [2007]

in vivo model of cardiac dilation

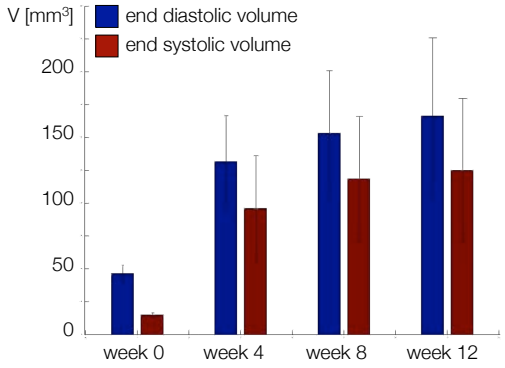

ejection fraction ↓ from 68.16% to 23.33%

doyle, sheikh, sheikh, cao, yang, robbins, wu [2007]

in silico prediction of cardiac dilation

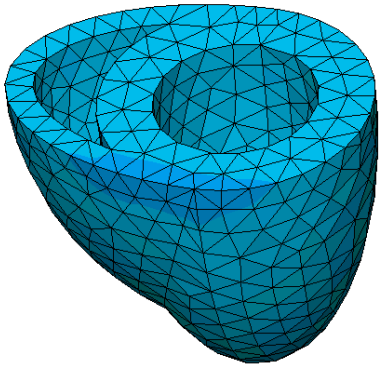

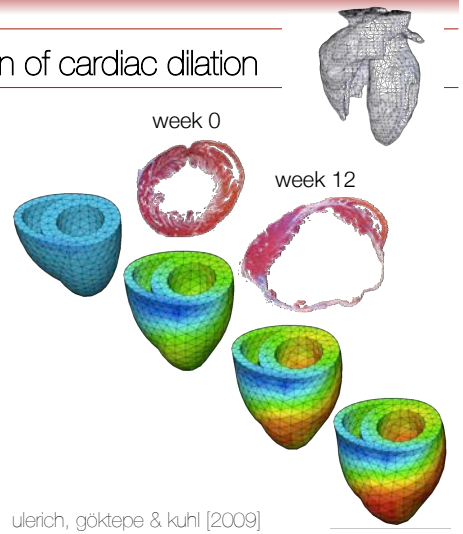

ulerich, göktepe & kuhl [2009]

doyle, sheikh, sheikh, cao, yang, robbins, wu [2007]

in vivo model of sarcomerogenesis

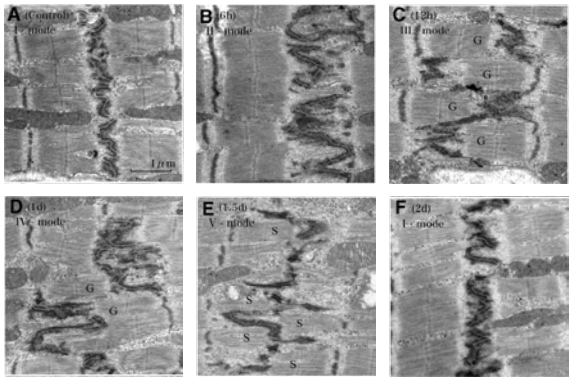

Figure 10. Ultrastructural changes of the intercalacted disk after volume overload. A Control. After 6 hours of volume overload, the ICD becomes thick with one-sarcomere-long interdigitations. B After 12 hours, the ICD is folded to form one-sarcomere-deep grooves and contra-grooves with short interdigitations. C At 1 day, interdigitations elongate up to one-sarcomere long in the folded ICD, D, so that the ICD broadens to ~two sarcomere wide. Grooves and contra-groves appear in this mode. At 1.5 days, the ICD is thin with mostly short interdigitations, but one-sarcomere-long interdigitations sporadically appear as spikes. E.There appear spaces surrounded by several spikes. At 2 days, the ICD is thin and flat with short interdigitaitons similar to those of controls, finishing one cycle of serial sarcomere addition.

yoshida, sho, nonjo, takahashi, kobayashi, kawamura, honma, komatsu, sugita, yamauchi, hosoi, ito, masuda [2010]

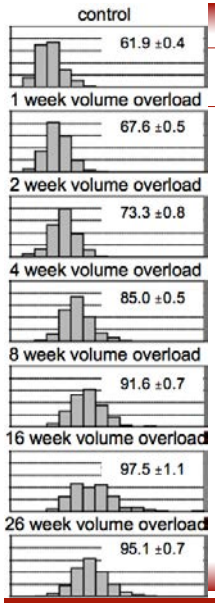

in vivo model of sarcomerogenesis

- **14% dilation** due to volume overload
- dilation by **cardiomyocyte elongation**
- elongation by **serial sarcomere deposition**
- sarcomere **number increases linearly** from 62 to 85
- sarcomere deposition **rate is linear** in weeks 1 to 4 decays smoothly to **saturation** at week 26

yoshida, sho, nonjo, takahashi, kobayashi, kawamura, honma, komatsu, sugita, yamauchi, hosoi, ito, masuda [2010]

strain-driven eccentric growth through sarcomerogenesis

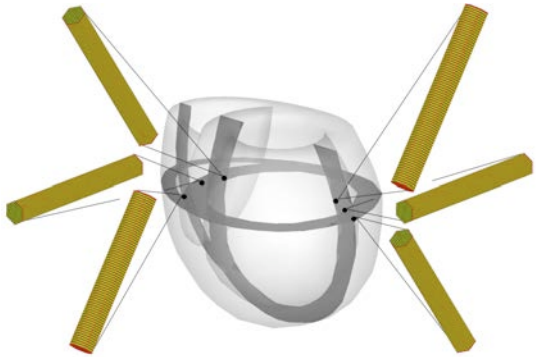

Figure 7. Strain-driven eccentric growth. Overall, eccentric growth is clearly hetergeneous with a transmural variation in serial sarcomere deposition. Cardiomyocytes in the endocardium, the inner wall, reach their maximum length of 150μm through the serial deposition of 25 additional sarcomere units of 2μm each. Cardiomyocytes in the epicardium, the outer wall, reach a stable state at a length of 130μm through the serial deposition of 15 additional sarcomere units. Eccentric growth along the septum is almost identical to eccentric growth along the free wall initiating an overall shape change from elliptical to spherical.

ocklenga, ablez, parker, kuhl [2010]

cardiac dilation - eccentric growth 37

case III - cardiac wall thickening

- chronic **wall thickening** at constant cardiac size
- wall thickness **increases from 1cm to 3cm**

- cardiomyocyte number remains constant ~6 billion
- cardiomyocyte diameter **increases from 15um to 40um**

- sarcomere number **increases in parallel**
- sarcomere length remains constant at 1.9-2.1um

opie [2003] maron, mc kenna [2003] kumar, abbas, fausto [2005]

cardiac wall thickening - concentric growth 38

case III - cardiac wall thickening

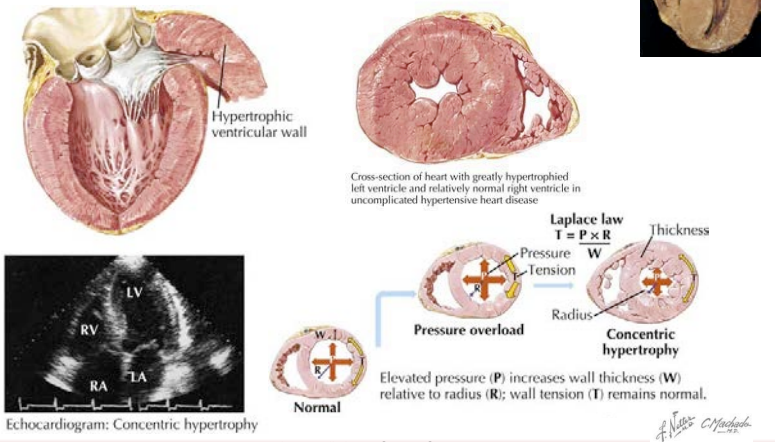

netter's cardiology [2010]

cardiac wall thickening - concentric growth 39

constitutive equations

- multiplicative decomposition
  $\boldsymbol{F} = \boldsymbol{F}^{\mathrm{e}} \cdot \boldsymbol{F}^{\mathrm{g}}$ with $\boldsymbol{F} = \nabla_{\boldsymbol{X}} \boldsymbol{\varphi}$
- growth tensor
  $\boldsymbol{F}^{\mathrm{g}} = \boldsymbol{I} + [\,\vartheta^{\mathrm{g}} - 1\,]\, \boldsymbol{s}_0 \otimes \boldsymbol{s}_0$
- evolution of concentric growth multiplier
  parallel sarcomere deposition rate
  $\dot{\vartheta}^{\mathrm{g}} = k^{\mathrm{g}}(\vartheta^{\mathrm{g}})\, \phi^{\mathrm{g}}(\boldsymbol{M}^{\mathrm{e}})$ with $k^{\mathrm{g}}(\vartheta^{\mathrm{g}}) = \frac{1}{\tau}\left[\frac{\vartheta^{\max} - \vartheta^{\mathrm{g}}}{\vartheta^{\max} - 1}\right]^{\gamma}$
- growth criterion
  $\phi^{\mathrm{g}} = \mathrm{tr}(\boldsymbol{M}^{\mathrm{e}}) - M^{\mathrm{e\,crit}}$

maximum parallel sarcomere deposition $\vartheta^{\max}$, sarcomere deposition time τ, deposition nonlinearity γ, critical pressure level $M^{\mathrm{e\,crit}}$

cardiac wall thickening - concentric growth 40

algorithmic treatment

given $\boldsymbol{F}$ and $\vartheta^{\mathrm{g}}_{\mathrm{n}}$	
initialize $\vartheta^{\mathrm{g}} \leftarrow \vartheta^{\mathrm{g}}_{\mathrm{n}}$	
local Newton iteration	
calculate growth tensor $\boldsymbol{F}^{\mathrm{g}} = \boldsymbol{I} + [\vartheta^{\mathrm{g}} - 1]\, \boldsymbol{s}_0 \otimes \boldsymbol{s}_0$	(51)
calculate elastic tensor $\boldsymbol{F}^{\mathrm{e}} = \boldsymbol{F} \cdot \boldsymbol{F}^{\mathrm{g}\,-1}$	(1)
calculate elastic right Cauchy Green tensor $\boldsymbol{C}^{\mathrm{e}} = \boldsymbol{F}^{\mathrm{e}\,\mathrm{t}} \cdot \boldsymbol{F}^{\mathrm{e}}$	(2)
calculate second Piola Kirchhoff stress $\boldsymbol{S}^{\mathrm{e}} = 2\,\partial\psi / \partial \boldsymbol{C}^{\mathrm{e}}$	(10)
check growth criterion $\phi^{\mathrm{g}} = \mathrm{tr}(\boldsymbol{C}^{\mathrm{e}} \cdot \boldsymbol{S}^{\mathrm{e}}) - M^{\mathrm{e\,crit}} \geq 0$?	(56)
calculate growth function $k^{\mathrm{g}} = [[\vartheta^{\max} - \vartheta^{\mathrm{g}}]/[\vartheta^{\max} - 1]]^{\gamma} / \tau$	(55)
calculate residual $\mathsf{R} = \vartheta^{\mathrm{g}} - \vartheta^{\mathrm{g}}_{\mathrm{n}} - k^{\mathrm{g}}\, \phi^{\mathrm{g}} \Delta t$	(58)
calculate tangent $\mathsf{K} = \partial \mathsf{R} / \partial \vartheta^{\mathrm{g}}$	(59)
update growth multiplier $\vartheta^{\mathrm{g}} \leftarrow \vartheta^{\mathrm{g}} - \mathsf{R} / \mathsf{K}$	
check convergence $\mathsf{R} \leq \mathrm{tol}$?	
calculate second Piola Kirchhoff stress $\boldsymbol{S} = \boldsymbol{F}^{\mathrm{g}\,-1} \cdot \boldsymbol{S}^{\mathrm{e}} \cdot \boldsymbol{F}^{\mathrm{g}}$	(17)
calculate Lagrangian moduli L	(18) with (19), (20), (53), (60)
push forward to Kirchhoff stress $\boldsymbol{\tau} = \boldsymbol{F} \cdot \boldsymbol{S} \cdot \boldsymbol{F}^{\mathrm{t}}$	(21)
push forward to Eulerian moduli $\mathbf{e} = [\boldsymbol{F} \,\overline{\otimes}\, \boldsymbol{F}] : \mathsf{L} : [\boldsymbol{F}^{\mathrm{t}} \,\overline{\otimes}\, \boldsymbol{F}^{\mathrm{t}}]$	(22)

Table 3. Algorithmic treatment of stress-driven transversely isotropic growth.

pathophysiology of cardiac wall thickening

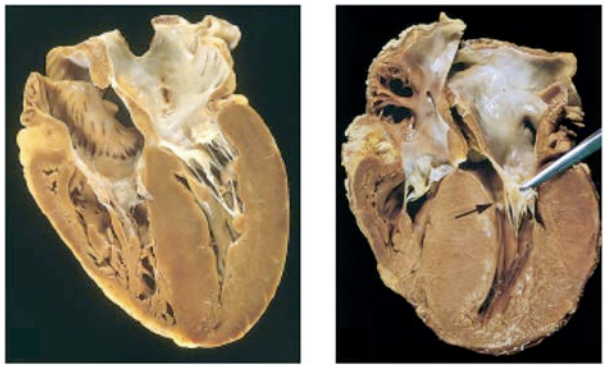

Figure 10. Stress-driven concentric growth , cardiac wall thickening, and transmural muscle thickening at constant cardiac size, reprinted with permission from Robbins & Cotran. Left ventricular outflow obstruction has caused pressure-overload hypertrophy associated with a significant wall thickening (left). A pronounced septal hypertrophy has caused the significantly thickened septal muscle to bulge into the left ventricular outflow tract (right).

cardiac wall thickening through stress-driven concentric growth

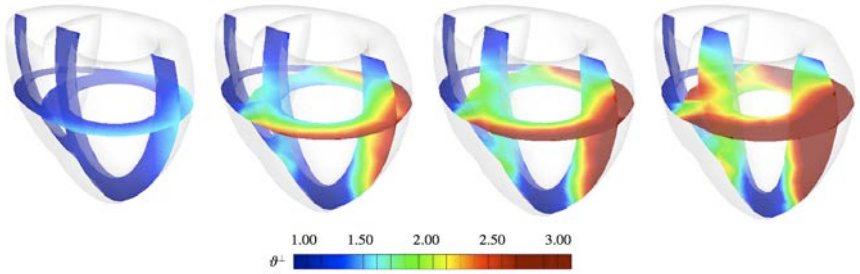

Figure 10. Stress-driven concentric growth. The concentric growth multiplier gradually increases from 1.00 to 3.00 as the individual cardiomyocytes grow concentrically. On the structural level, concentric growth manifests itself in a progressive transmural wall thickening to withstand higher blood pressure levels while the overall size of the heart remains virtually unaffected. Since the septal wall receives structural support through the pressure in the right ventricle, wall thickening is slightly more pronounced in the free wall where the wall stresses are higher.

cardiac wall thickening through stress-driven concentric growth

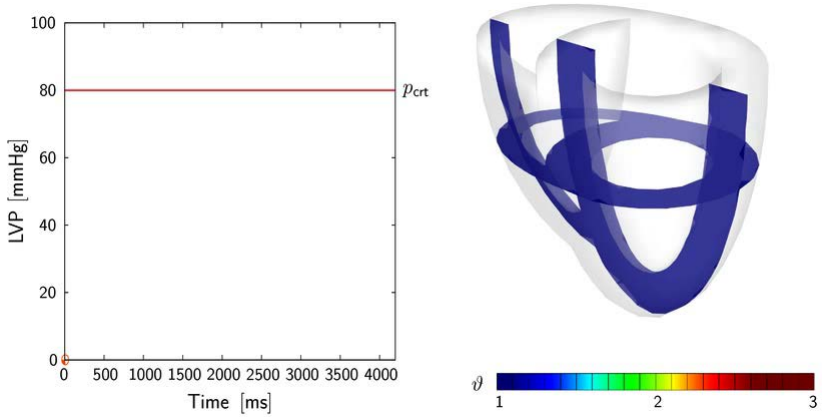

stress-driven concentric growth through sarcomerogenesis

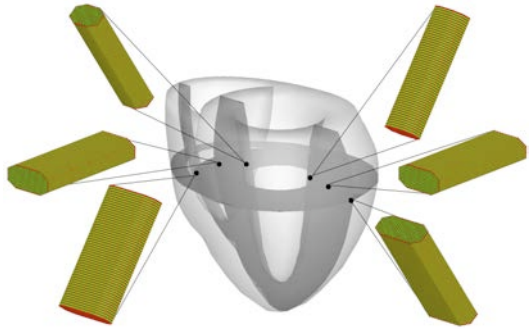

Figure 9. Stress-driven concentric growth. Concentric growth is clearly heterogeneous with a transmural variation in parallel sarcomere deposition. Cardiomyocytes in the endocardium, the inner wall, reach a stable state at a thickness of 31.4μm through the parallel deposition of 84 additional sarcomere units. Cardiomyocytes in the epicardium, the outer wall, reach their maximum thickness of 50μm through the parallel deposition of 182 sarcomere units. Concentric growth at the free wall is slightly more pronounced than at the septum.

göktepe, abilez, parker, kuhl [2010]

cardiac wall thickening - concentric growth 45

systemic vs pulmonary hypertension

Figure. Stress-driven concentric growth, cardiac wall thickening, and transmural muscle thickening at constant cardiac size. Left ventricular wall thickening in response to systemic hypertension (left) from Kumar, Abbas, Fausto [2005]. Right ventricular wall thickening in response to pulmonary hypertension (right), from Padera.

rausch, dam, göktepe, abilez, kuhl [2010]

cardiac wall thickening - concentric growth 46

systemic vs pulmonary hypertension

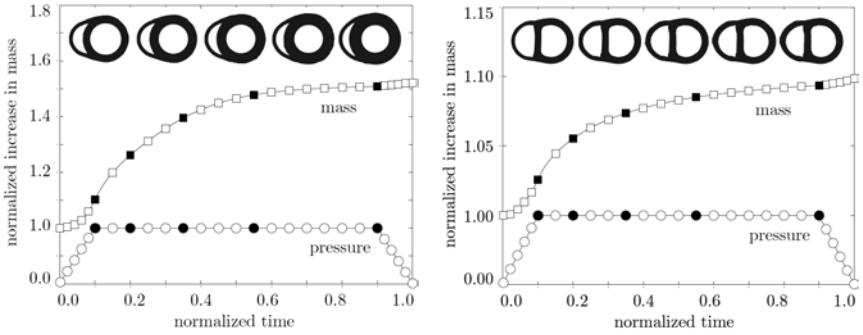

cardiac mass increases more
in systemic (+50%) than in pulmonary (+10%) hypertension

rausch, dam, göktepe, abilez, kuhl [2010]

cardiac wall thickening - concentric growth 47

systemic vs pulmonary hypertension

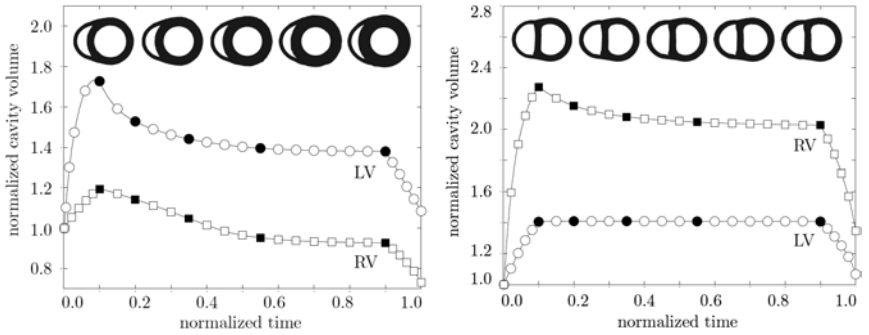

cavity volumes decrease significantly
in both systemic and pulmonary hypertension

rausch, dam, göktepe, abilez, kuhl [2010]

cardiac wall thickening - concentric growth 48

systemic hypertension - LV wall thickening

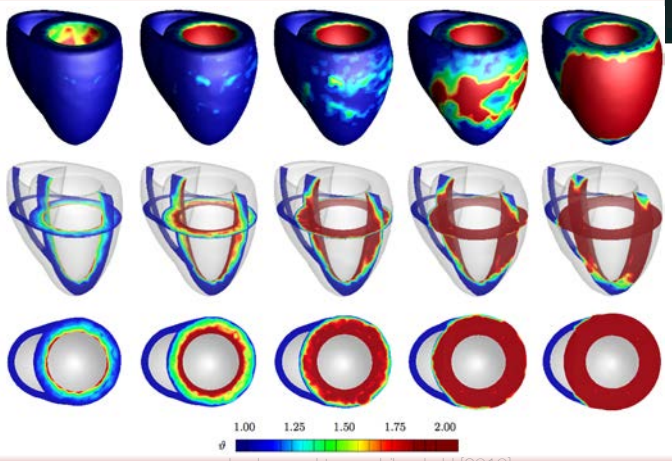

rausch, dam, goktepe, abilez, kuhl [2010]

cardiac wall thickening - concentric growth 49

pulmonary hypertension - RV wall thickening

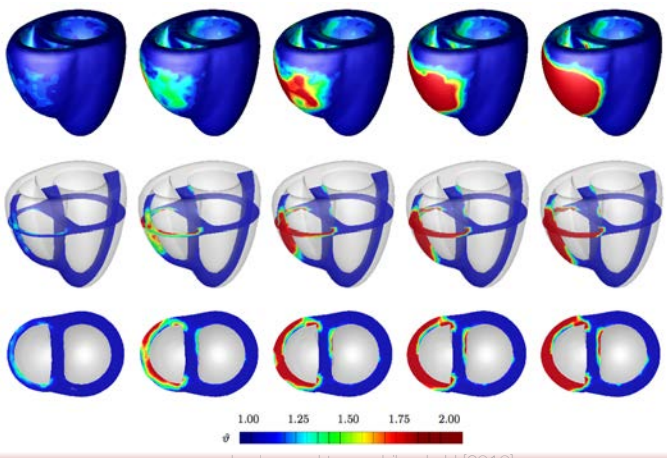

rausch, dam, goktepe, abilez, kuhl [2010]

cardiac wall thickening - concentric growth 50

the living heart project

SIMULIA

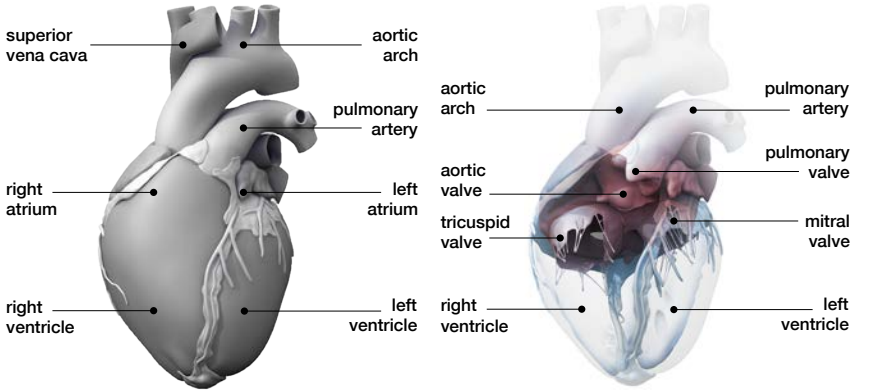

anatomic and circulatory model of the human heart created from computer tomography and magnetic resonance images. the model displays the characteristic anatomic and circulatory features of the human heart; adopted with permission from zygote.

towards realistic human heart modeling 51

the living heart project

SIMULIA

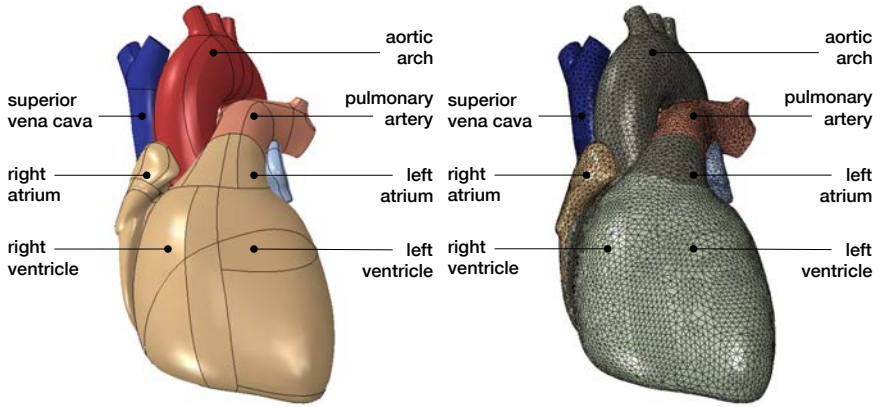

solid model and finite element model of the human heart discretized with 208,561 linear tetrahedral elements, 47,323 nodes, and 189,292 degrees of freedom, of which 47,323 are electrical and 141,969 are mechanical.

towards realistic human heart modeling 52

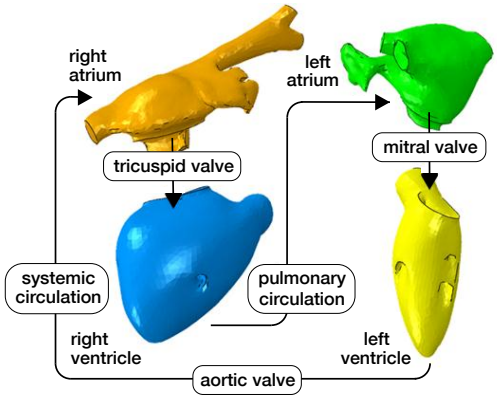

blood flow model of the human heart with surface-based fluid cavity representation of the right atrium, right ventricle, left atrium, and left ventricle connected through viscous resistance models of windkessel type for the tricuspid valve, pulmonary circulation, mitral valve, aortic valve, and systemic circulation.

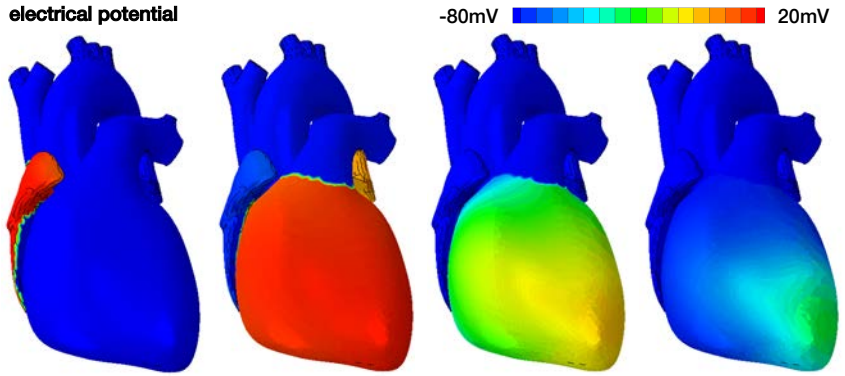

spatio-temporal evolution of electrical potential across the human heart. during systole, the heart depolarizes rapidly from -80mV to +20mV. during diastole, the heart repolarizes gradually from +20mV to -80mV.

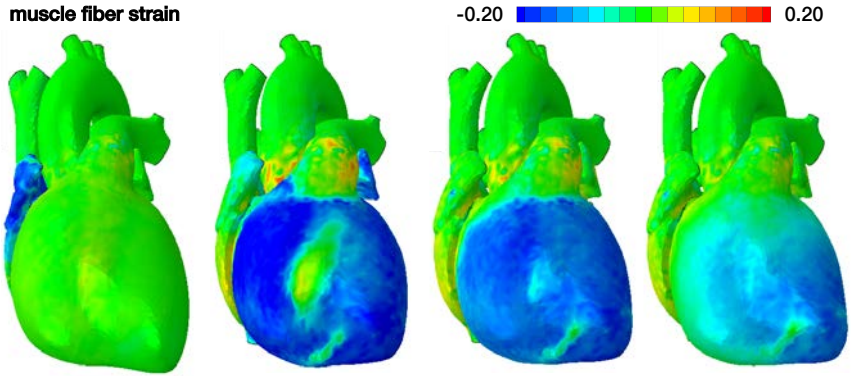

spatio-temporal evolution of muscle fiber contraction across the human heart. during systole, the muscle fibers contract and shorten up to 20\% to induce ventricular ejection. during diastole, the muscle fibers relax and relengthen to their initial length to induce ventricular filling.

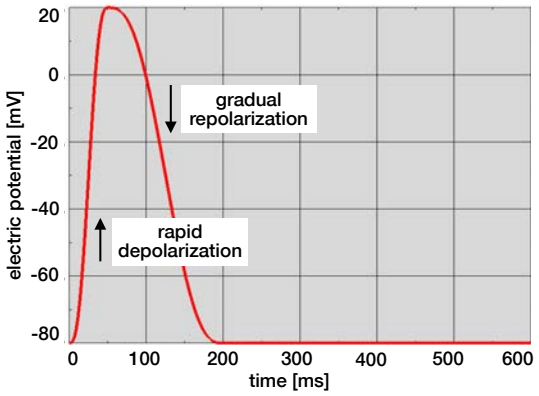

temporal evolution of the electrical potential. During excitation, cardiac cells rapidly depolarize and the electrical potential increases from -80mV to +20mV within the order of milliseconds. During relaxation, cardiac cells gradually repolarize and return to the stable baseline state at -80mV.

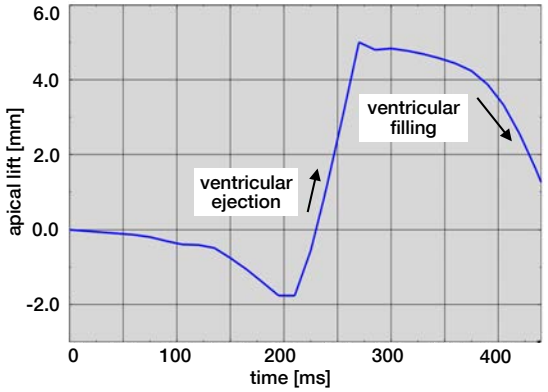

temporal evolution of the apical lift. during ventricular ejection, the apex moves rapidly upward towards the base and the ventricles shortens by 7mm along the long axis. during ventricular filling, the apex gradually returns to its initial position as the heart muscle relaxes.

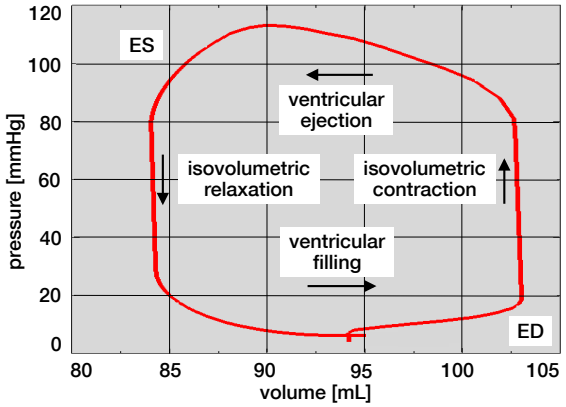

pressure-volume loop of the human heart with characteristic phases of ventricular filling, isovolumetric contraction, ventricular ejection, and isovolumetric relaxation. the enclosed area characterizes the work performed throughout the cardiac cycle.